LSTM-Based Multi-Link Prediction for mmWave and Sub-THz Wireless Systems

Syed Hashim Ali Shah, Manali Sharma and Sundeep Rangan
NYU WIRELESS, Tandon School of Engineering, New York University, Brooklyn, NY 11201
e-mail: {s.hashim,manali.sharma,srangan}@nyu.edu

***Abstract*—A key challenge in mmWave systems is the rapid variations in channel quality along different beam directions. MmWave links are highly susceptible to blockage and small changes in the orientation of the device or appearance of blockers can lead to dramatic changes in link quality along any given direction. Many low-latency applications need to accurately predict link quality from multiple directions and multiple cells. This paper presents a novel long short term memory (LSTM)-based method for predicting multi-directional link quality in mmWave systems. The method is validated on two problems: A realistic simulation of multi-cell link tracking in an environment with randomly moving human and vehicular blockers at 28 and 140 GHz, and beam prediction in a real indoor setting at 60 GHz.**

***Index Terms*—Millimeter wave; LSTM; machine learning; cellular wireless**

I. Introduction

Millimeter wave (mmWave) bands and other frequencies above 6 GHz have emerged as key components of emerging fifth generation (5G) cellular standards [1]–[3]. The vast available bandwidths in these frequencies provide both lower latency and high throughput. These capabilities are hoped to enabled new applications in vehicle to everything (V2X), robotics, drones and other areas.

However, one of the key challenges of supporting reliable communication in mmWave bands is the high sensitivity of signal blockages caused by humans, hand and many common building materials [4]–[6]. Thus, small changes in the orientation of the device or appearance of blockers can result in a rapid degradation of link quality in any given direction. mmWave systems thus need to track and predict link quality along multiple directions to sustain the link.

In addition, most mmWave systems rely on dense cell deployments combined with multi-connectivity to provide macro-diversity resistance to blockage [7]. Multi-connectivity can be supported via carrier aggregation [8] where a mobile (UE) can be simultaneously connected to multiple cells. While carrier aggregation was introduced in 4G systems, its use in 5G mmWave networks presents an additional challenge: the mobile must track link quality from multiple cells *and* multiple directions.

This paper considers a general multi-link prediction problem where links can either be from different cells or different directions from a cell. The problem is to estimate future link quality from past (possibly noisy or incomplete) measurements. Traditional statistical prediction approaches are difficult, since link statistics are complex and difficult to estimate. We thus propose a machine learning approach. Specifically, we formulate the multi-link prediction problem as a vector-valued sequence-to-sequence problem. Recurrent neural networks (RNNs) in deep learning are commonly used for such problems [9], [10]. In this work, we use a well-known RNN called Long Short Term Memory (LSTM). LSTMs can capture long-term dependencies and have been successful in a range of problems, particularly in natural language processing, speech recognition and robotics.

Previous work on single link quality predictions have been done for sub 6 GHz frequency for a vehicular scenario in [11]. Work on link prediction based on LTE and WiMax measurements has been done in [12]. CSI estimation using deep learning has also been addressed in [13] and tested on sub 6 GHz measurements. For mmWave networks, [14] uses Gated Recurrent Unit (GRU) for single link prediction and discusses applications like blockage prediction and proactive hand-over. This work goes beyond these results in studying multi-link problems, which are essential in the mmWave range. The prediction capability will help in processes like proactive beam switching, handovers and uses in V2X, robotics and drone communications.

The paper is organized as follows. We describe the problem formulation and use cases in Section II. We will setup an LSTM network for multi-link prediction and test it on simulations at mmWave and sub THz frequencies based on 3GPP channel model with mobile blockers. The prediction power of LSTM will be compared with one of the generic prediction methods (moving average). We will then test the prediction ability of LSTM on real life measurement data from a beamformed system operating at 60 GHz with multiple links. It is observed that the LSTM prediction performance is better than that of the conventional moving average for both simulations and measurement data. It is also established that LSTM prediction is more robust to carrier frequency as compared to a linear estimator like moving average.

II. Problem Formulation and Use Cases

A. Multi-Link Prediction Problem

Assume time is divided into discrete intervals of period T and we index the intervals $t = 0, 1, 2, \ldots$. We assume there are K *links*. In a single cell scenario, there could be one link for each direction. In a multi-cell scenario, there could be one link for each cell or for each direction and cell. In any case,

978-1-7281-5089-5/20/$31.00 ©2020 IEEE

we let $\gamma(k,t)$ be some measure of channel quality on link $k = 1,2,\ldots,K$ in time interval t. The channel quality could be the SNR for a flat fading channel or wideband SNR or mutual information for a frequency selective fading channel. With any definition, the link quality is a vector-valued process with K values at each time. The major difference between multi-link and single link predictions is that instead of a single value prediction, we have to do a K dimensional vector prediction.

We consider a one-step ahead prediction problem, where the goal is to estimate the link quality $\gamma(k,t)$ from channel quality measurements from past time steps: $\gamma(\ell,s)$ for $s < t$ and $\ell = 1,\ldots,K$. In some cases, you may only have measurements on a subset of the links.

This scenario can be naturally applied to link tracking in the 5G NR standard [3]. First consider tracking the link quality from a single cell. Suppose that the transmitter has N_{tx} TX directions, and the receiver has N_{rx} RX directions so there is exactly one codeword in each orthogonal spatial degree of freedom. Hence there is a total of $K = N_{tx}N_{rx}$ links. To track link quality, each 5G cell periodically transmits a set of synchronization signal bursts (SSBs) [15]. Let T be the SSB period (typically $T = 20$ ms) and assume the cell transmits one SSB in each of the N_{tx} directions. Now, suppose that the UE has a fully digital receiver. Then, in each SSB period T, the UE can measure the channel quality $\gamma(k,t)$ in all TX-RX direction pairs. If the UE performs the beamforming in analog (e.g. via RF phase shifters), the UE can measure some subset of the directions k in each time t. In either case, the one-step ahead prediction problem is to estimate the directional link quality vector one SSB period in advance. The problem can be extended to multiple cells by tracking one channel quality for each TX-RX pair for each cell.

B. Use Cases

Several important applications like V2X, robotics/Internet of things (IoT), drone communications, etc. require reliable tracing of time-varying link quality.

For example in a vehicular setup the reliability of the mmWave link is compromised due to beam alignment errors and blockages [16]. As most blockages occurring in V2X environments are either caused by the terrain or building infrastructure, they do not alter frequently. Thus, the predicted channel characteristics can be relied upon because the training and test environments are very similar. Moreover, these parameters can be used to detect beam or link failures and trigger early beam switching or handovers (HO).

In robotics and drones communication, mobile units require huge amounts of processing power to perform mechanical tasks such as balancing, moving, etc. Since the computational power that these mobile robots or drones can carry is limited by the power/energy demands of high-end computing systems such as CPUs or GPUs, these large computational units are moved to the edge server. But the latency requirements for transmission between the robot/drone and the edge server are extremely strict. [17] shows that a communication link serving a drone is unable to support the application when the round trip delay exceeds 5 ms. For example assume that the latency of a communication link is severely effected by a blockage event. If this event can be predicted earlier, a drone/robot can alter the robot kinematics[18] or do a handover beforehand such that the link latency does not deteriorate. The predicted channel state information specific to beams can be useful in determining the most reliable link from a drone/robot to an access point hence catering to the requirements of the given applications.

In the cellular context, "Early handover" has been actively discussed as a solution to the challenges posed by mobility in 5G NR. It is popularly known as conditional handover (CHO). [19],[20] define conditional handover as an additional step before the handover procedure where the UE initiates a CHO request to multiple target cells based on an early trigger condition. On reception of this request the target cells request for the UE context from the source BS to prepare for actual HO [21]. 3GPP RAN2#106 meeting agreements state that the value of trigger condition for CHO would be defined statically and stay fixed. This opens the CHO procedure to major challenges such as unnecessary measurement reports, frequent *RRCReconfiguration* failures etc., which in-turn lead to more latency. Thus, SNR prediction and thereby RSRP values for the serving BS and the best beam of target BSs can be very useful in determining the best candidates for CHO in advance. The predicted channel state can help create a more accurate trigger condition for CHO, which can further lead to reduced handover delay.

In the rest of this paper, we show how an LSTM network can help with the multi-link prediction problem, which will help us cater the communication requirements of the applications mentioned above.

III. Proposed LSTM Network

The one-step ahead prediction problem can be naturally formulated as a sequence-to-sequence problem. At each time step t, we will use the notation $\gamma^{(t)}$ to denote the K-dimensional vector with components $\gamma(k,t)$, $k = 1,\ldots,K$. For simplicity, we will assume we measure the directional quality on all links at each time. We then take the past values of $\gamma^{(t)}$ as the input sequence and have it generate an output sequence $\gamma^{'(t)}$ representing the predicted value of the vector $\gamma^{(t)}$. If the model is strictly causal, so that $\gamma^{'(t)}$ only depends on past values $\gamma^{(s)}$ for $s < t$, then the network will be performing prediction. The prediction performance as the function of the number of timesteps is left for future work.

In this work, we consider an LSTM [9], which is widely used for sequence-to-sequence problems with long-term memory. We use the standard LSTM:

$$g^{(t)} = \phi(W^{g\gamma}\gamma^{(t)} + W^{gh}h^{(k,t-1)} + b_g) \quad (1)$$

$$i^{(t)} = \sigma(W^{i\gamma}\gamma^{(t)} + W^{ih}h^{(k,t-1)} + b_i) \quad (2)$$

$$f^{(t)} = \sigma(W^{f\gamma}\gamma^{(t)} + W^{fh}h^{(k,t-1)} + b_f) \quad (3)$$

$$o^{(t)} = \sigma(W^{o\gamma}\gamma^{(t)} + W^{oh}h^{(k,t-1)} + b_o), \quad (4)$$

$$s^{(t)} = g^{(t)} \odot i^{(t)} + s^{(k,t-1)} \odot f^{(t)}) \quad (5)$$

$$h^{(t)} = \phi(s^{(t)}) \odot o^{(t)} \quad (6)$$

$$\gamma'^{(t)} = s^{(t)} \odot o^{(t)}) \quad (7)$$

The network maps the input sequence $\gamma^{(t)}$ to the output prediction $\gamma'^{(t)}$ through a number of interval or hidden variables that have various functions to model past dependencies in the data. The signal flow is illustrated in Fig. 1. The hidden variables are the forget gate $f^{(t)}$, input gate $i^{(t)}$, input node $g^{(t)}$, hidden layer $h^{(t)}$, output gate $o^{(t)}$ and memory cell state $s^{(t)}$ [22], [23]. The input gate decides whether the current incoming data is contributing new information to the network. The forget gate flushes out unwanted data from the memory. The output gate dictates what to show at the network output.

Each interval variable is the output of a linear combination of the hidden state h^t and input γ^t followed by an activation function. The activation function is generally either a *sigmoid* ($\sigma(\cdot)$) or *tanh* ($\phi(\cdot)$). We use the notation that W^{xy} is the weight matrix between x and y. b_x is the bias of the gate or node x and $\odot$ translates to pointwise multiplication. For convenience, we use the following short-hand:

$$\gamma'(k,t) = L(\gamma(k,t)), \quad (8)$$

where $L(\gamma(t))$ means the input has been passed through (1)-(7).

The complexity of the LSTM network is determined on the number of units of the different types. The dimensions can be determined via cross-validation. For a given set of internal dimensions during the training phase, the LSTM network learning optimizes all the weights and biases of all the layers, nodes and gates in such a manner that the loss is minimized. For this work, we will be using mean squared error (MSE)

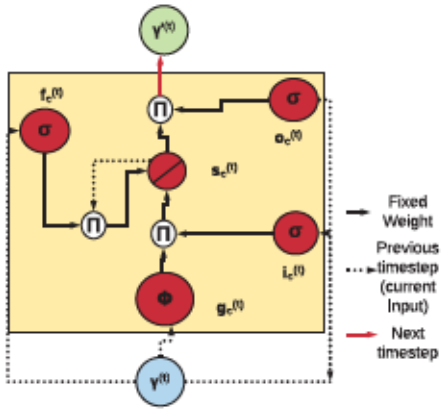

Fig. 1: Process diagram of a memory cell of an LSTM network based on the (1)-(7). Figure from [22].

as the loss function. Mathematically, for the total number of samples $N \times K$, MSE is given by,

$$MSE = \frac{1}{NK}\sum_{n=1}^{N}\sum_{k=1}^{K}(\gamma'(k,n) - \gamma(k,n))^2. \quad (9)$$

IV. Experiments

We evaluate the LSTM learning of a multi-link model on two datasets. The first is synthetic, and the second is from real mmWave measurements.

A. Simulated multi-cell tracking with blockers

End-to-end communication network simulations are used to generate the dataset on which the LSTM link quality prediction is tested. 100 channel trajectories are generated using the 3GPP channel model [24] at 28 GHz and 140 GHz[1]. The BSs are dropped randomly on a $200 \times 200\text{m}^2$ grid, in such a way that the cell radius for each BS is 100m. The number of antennas at BS is $M_b = 64(256)$ and the number of antennas at UE is $M_u = 8(64)$ for 28 GHz (140 GHz). BS and UE codebooks have M_b and M_u beams respectively. The simulated time T_o, for each trajectory is 100 seconds.

The UE has a height of 1.7 m and is dropped randomly within the BS grid. We do not consider the impact of the array geometry for the sake of simplicity. In this static model, the UE tracks one direction for each cell, which we assume it pre-determines from beam search.

Blockers are then deployed within the cell using a Poisson point process with density λ_b. The blockers can either be human or vehicular, with equal probability. The blockers are modeled as a rectangular screen with specific height and width; these numbers are provided by 3GPP. The heights of the human(vehicular) blockers are 1.7m(1.4m) while the widths are 0.3m(4.5m). The blockage loss is modeled by the Double Knife Edge Diffraction (DKED) model provided by 3GPP.

The blockers follow random waypoint model. Over all the trajectories, the human(vehicular) blockers have their velocities uniformly distributed between $0-3$ km/hr (0-100 km/hr). For each channel trajectory, let $x_j(0) \in \mathbb{R}^2$ be the position of the j-th blocker at time $t = 0$. A destination point $d_j \in \mathbb{R}^2$ is generated randomly within the cell for the blocker. d_j is a 2D uniform random variable, which is restricted inside the BS grid. As time progresses, the blocker moves toward the destination with velocity $\dot{x}$. Let Δt be the sampling interval for simulation. Then the evolution of the position of the blocker follows the equation:

$$x_j(t) = x_j(t-1) + \dot{x}\Delta t \quad (10)$$

Δt is chosen to be $20ms(T)$ since it corresponds to the value of synchronization signal burst (SSB) period in the most recent 3GPP specification report [25], meaning the UE gets an update of the link quality every 20 ms.

[1]The specifications of the 3GPP channel model in [24] are valid up to 100GHz only, we continue to use it even for 140GHz because of the absence of standardized channel models for the spectrum above 100 GHz

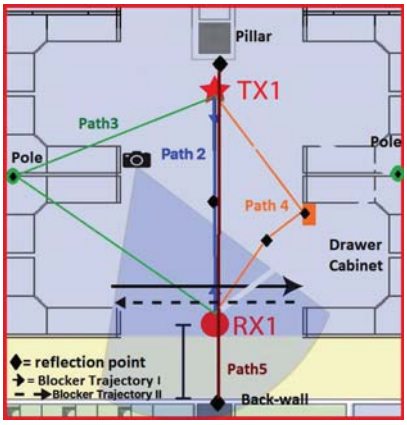

Fig. 2: Venue for experimental setup with multiple paths(links) and human blocker trajectories. (LOS path not shown). The start point of blocker is tail of the arrow and end point is head of the arrow.

Parameters	28 GHz	140 GHz
Scenario	UMi	
M_u	8	64
M_b	64	256
Bandwidth	400MHz	1.6GHz
N	9	
UE height	1.7m	
BS height	10 m	
Sampling interval	20 ms	
Temperature	298 K	
Cell radius, r	100 m	
Blocker density, λ_b	0.01 m^{-2} [27]	
Blocker height	1.4 m (Vehicular), 1.7 m (Human)	
Blocker width	4.8 m (Vehicular), 0.3 m (Human)	
Blocker speed	0-28 m/s (0-100 km/h)[Vehicular] 0-1 m/s (0-3 km/h)[Human]	
Transmitted Power	23dBm [28]	
Noise Figure	9dB [29]	

TABLE I: Values of different parameters for the generation of channel trajectories

Once $x_j(t) = d_j$, d_j is reset along with the velocities of the blockers. This process is repeated until the running time of the simulation for the given trajectory is over. Both kinds of blockers follow a similar mobility model; they are only distinguished by the distribution of their velocities.

List of parameters for generating the channel trajectories has been provided in Tab. I. Similar simulation setup was done in [26].

B. Indoor Multi-Direction Tracking with Real Data

In this test, we evaluate the link tracking on real indoor measurements using a phased-array system in [5], [30]. The operating frequency of the system is 60 GHz, the frequency for mmWave WiFi (802.11ad and 802.11ay). The TX and RX both have 12 antenna elements and have predefined codebooks (12 beams at TX and 12 at RX) for beamforming (a total of 144 beam pairs).

The transmitter (TX) and receiver (RX) have been placed in an ideal cubicle jungle inside an office. The top-view of the measurement venue is shown in Fig. 2. The distance between TX and RX is 5m. The TX and RX are aligned in such a way that they are facing each other. The TX is located at a height of 2.63m which is very close to the ceiling. The purpose of putting TX at such a height is replicating a real-life access point. The RX is located at a height of 1.37m from the ground[2], which is done to replicate a human holding a cell phone or any other communication device. The measurement venue consists of many objects capable of reflection like cubicle walls, pillars, metal shelving, drawers, floor etc.

We could use the link tracking algorithm to track all 144 TX-RX direction pairs. However, to simplify the problem, we pre-process the data to identify a small number of dominant paths and then track the link qualities on these directions. This method would work in a quasi-static environment where the only variations in link quality are caused by blockers.

The paths are determined by the algorithm given in [31]. The dominant paths discovered by the algorithm are shown in Fig. 2. As shown there is one LOS path and 4 NLOS paths for a total of $K = 5$ links. For each path (link), we identify the best TX/RX transmit/receive direction and analyze the received power on the identified direction. So the nature of multi-link tracking is a bit different from that of simulated mult-cell tracking. In simulations, we predict on one link from each BS (9 BS in total) but for measurements, we predict on 5 links from a single TX (is analogous to BS of simulations).

Fig. 2 also shows two blocker trajectories, in which the Rx is blocked by human blocker moving in the direction shown. The data from one of these trajectories will be chosen as training data for the LSTM network and the other trajectory will be used to test the prediction power of the LSTM network. The evolution of power for all the paths with blocker trajectory I can be observed in Fig. 3. Each sample of data is 3.2ms apart and the total number of samples for each blocker trajectory are 1750. In case of blocker trajectory I, the blocker moves from left to right as seen in Fig. 2 with a distance of 1m from the Rx, in case of blocker trajectory II, the blocker moves from right to left with a distance of 30 cm from the Rx causing a different kind of blockage event as compared to blocker trajectory I.

V. Results and Discussion

We discuss the performance of the LSTM network for both tests. For both tests, we report the RMSE, the root mean squared error (in dB). The parameters for creation and training of the LSTM network are given in Table II. The suitable values have been selected from [11], [12].

A. Simulated multi-cell tracking with blockers

We proceed to analyze the performance of the multi-link prediction using LSTM on simulation data. For each channel

[2]It should be noted that measurement were performed before hand so the data available is only for the heights mentioned. The camera in the Fig 2 was placed to observe the motion of blocker with live measurements and does not play any role in the current analysis

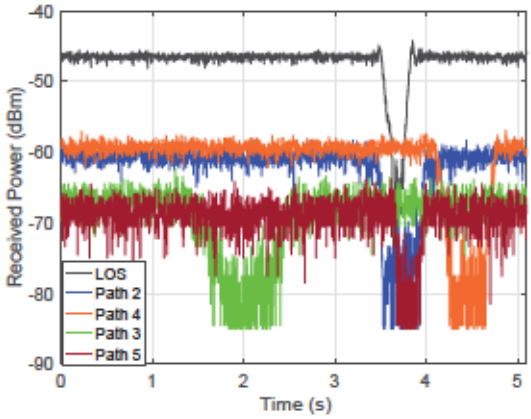

Fig. 3: Evolution of the received power with time, on all links for the measurement setup with blocker trajectory I

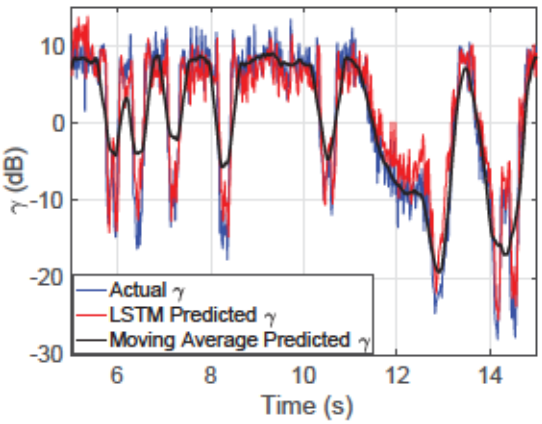

Fig. 4: Prediction of SNR using LSTM network vs moving average

trajectory generated, we use 50% of the data for training and the rest of the data is for testing purposes. For example each channel trajectory has a simulation time of $T_o = 100s$ sampled at $T = 20ms$, meaning we will have a total of $N = 5000$ samples. $N_{tr} = 2500$ of these samples will be used for training the LSTM network and $N_{ts} = 2500$ will be used to test the prediction capability of the LSTM network.

We compare the prediction capability of the LSTM with a simple linear moving average. We use a moving average of a sliding window of M samples to predict the future values. The value of SNR $\gamma_m^{(k,t_o)}$ on kth links with sample of interest at time t_o is predicted by moving average using the equation:

$$\gamma_m^{(k,t_o)} = \frac{1}{M} \sum_{j=t_o-M-1}^{t_o-1} \gamma^{(k,j)} \tag{11}$$

The LSTM network is designed to predict one timestep ahead meaning we will get the prediction of the multi-link SNR after $T = 20$ ms. The visualization of the LSTM prediction during testing phase for one BS for a single trajectory at 28 GHz is shown in Fig. 4. The correspondence between the actual γ and predicted γ' can clearly be observed. The intermittency of the channel is also predicted by the LSTM network which the moving average fails to capture. Blockage events can also be observed from the figure and it can be seen that LSTM network is also able to predict these events.

Table III shows how the prediction performance of LSTM compares to moving average method [3]. The values of RMSE shown in the table are over the total 100 channel trajectories

[3]The sample code for multi-link implementation using LSTM can be found at *https://github.com/shaspi/LSTM-Based-Multi-Link-Prediction-for-mmWave-and-Sub-THz-Wireless-Systems*

Parameter	Value	**Parameter**	Value
Loss	MSE	**Lookback**	20
Optimizer	Adam	**Batch Size**	10
Training Epochs	50	**Normalization**	minmax

TABLE II: LSTM network parameters

generated from simulation at 28 GHz and 140 GHz. There is a difference of about 1 dB in performance of LSTM at 28 GHz and 140 GHz while the difference is 4 dB for moving average. This change is because the channel becomes more and more intermittent as the frequency is increased. The comparison of LSTM with moving average at respective carrier frequency shows that the difference increases from 5 dB at 28 GHz to 9 dB at 140 GHz. It can clearly be seen that LSTM has a better prediction capacity as compared to moving average. Another interesting point worth noting is that the LSTM prediction is much more robust to the carrier frequency as compared to the moving average.

B. Measurement Data

In this subsection, we will measure the predicting capacity of the LSTM network on real measurement data obtained from measurement setup in section IV-B. The quantity of interest

Frequency	**Method**		**Mean RMSE (dB)**
28 GHz	**LSTM**	Train	4.65
		Test	4.60
	Moving Average		10.29
140 GHz	**LSTM**	Train	5.58
		Test	5.46
	Moving Average		14.29

TABLE III: Prediction performance of LSTM vs moving average at 28 GHz and 140 GHz simulated data

Frequency	**Method**		**Mean RMSE (dB)**
Case I	**LSTM**	Train	2.11
		Test	2.84
	Moving Average		3.74
Case II	**LSTM**	Train	2.09
		Test	3.14
	Moving Average		4.13

TABLE IV: Performance of LSTM and moving average prediction on measurement data for both cases

in this case will be the received power which in turn can be translated into SNR. We will perform prediction testing on experimental data in two cases, which will be differentiated on the basis of training data. In case I, we will train the LSTM network on the data obtained from blocker trajectory I, and testing will be performed on data from blocker trajectory II. In case II, training will be done on blocker trajectory II and testing will be done on blocker trajectory I. It is to be noted that blocker trajectories should not be confused with cases. The parameters used for training the LSTM network are same given in table II except for the training epochs since the size of the data is now smaller compared to the simulation case. The difference between the blocking trajectories is the direction of motion and the distance of the blocker from the Rx. The data is downsampled by a factor of 6 so that the sampling interval matches that of simulations. The LSTM network predicts one timestep ahead $T = 19.2\text{ms}$. The results for the train and test prediction for the LSTM network and the moving average method have been summarized in table IV .

We can see from table IV that the RMSE values are approximately the same magnitude for case I and case II. The RMSE is expected to be better than simulation data since there are a lot of random events, for example random blockages,in simulation which the network needs to take into account for accurate prediction. In both the cases, the LSTM predictor outperforms the moving average by a margin of 1 dB.

VI. Conclusions

Link prediction in the mmWave and sub-THz frequencies requires predicting link quality from multiple cells and multiple directions. Classical statistical prediction methods for link quality evaluation are difficult since the underlying process has complex dependencies in time and across links. We propose an LSTM method and evaluate the technique and both realistic multi-cellular simulations at 28 and 140 GHz and actual indoor data at 60 GHz. The results show that LSTMs can offer significantly better link prediction performance than simple baseline linear estimators.

Acknowledgements

This work was supported by the National Science Foundation under Grants 1302336, 1564142, and 1547332, NIST, SRC and the industrial affiliates of NYU WIRELESS.

References

[1] S. Rangan, T. S. Rappaport, and E. Erkip, "Millimeter-wave cellular wireless networks: Potentials and challenges," *Proc. IEEE*, vol. 102, no. 3, pp. 366–385, Mar. 2014.

[2] T. S. Rappaport *et al.*, "Millimeter Wave Mobile Communications for 5G Cellular: It Will Work!" *IEEE Access*, vol. 1, pp. 335–349, May 2013.

[3] 3GPP, "TS 38.300 NR; overall description; stage-2."

[4] T. S. Rappaport *et al.*, *Millimeter Wave Wireless Communications*. Pearson Education, 2014.

[5] C. Slezak *et al.*, "Empirical effects of dynamic human-body blockage in 60 GHz communications," *IEEE Commun. Mag.*, vol. 56, no. 12, pp. 60–66, 2018.

[6] T. Bai and R. W. Heath, "Coverage analysis for millimeter wave cellular networks with blockage effects," in *Proc. IEEE Global Conference on Signal and Information Processing*. IEEE, 2013, pp. 727–730.

[7] J. Choi, "On the macro diversity with multiple bss to mitigate blockage in millimeter-wave communications," *IEEE communications letters*, vol. 18, no. 9, pp. 1653–1656, 2014.

[8] G. Yuan *et al.*, "Carrier aggregation for LTE-advanced mobile communication systems," *IEEE communications Magazine*, vol. 48, no. 2, pp. 88–93, 2010.

[9] S. Hochreiter and J. Schmidhuber, "Long short-term memory," *Neural Computation*, vol. 9, pp. 1735–1780, 1997.

[10] C. E. Zachary C. Lipton, John Berkowitz, "A critical review of recurrent neural networks for sequence learning," *ArXiv*, 2015.

[11] J. Joo *et al.*, "Deep learning-based channel prediction in realistic vehicular communications," *IEEE Access*, vol. 7, pp. 27 846–27 858, 2019.

[12] J. D. Herath, A. Seetharam, and A. Ramesh, "A deep learning model for wireless channel quality prediction," in *ICC 2019 - 2019 IEEE International Conference on Communications (ICC)*, May 2019, pp. 1–6.

[13] C. Luo *et al.*, "Channel state information prediction for 5g wireless communications: A deep learning approach," *IEEE Transactions on Network Science and Engineering*, pp. 1–1, 2018.

[14] A. Alkhateeb, I. Beltagy, and S. Alex, "Machine learning for reliable mmwave systems: Blockage prediction and proactive handoff," *Proc. IEEE Global Conference on Signal and Information Processing (GlobalSIP)*, pp. 1055–1059, 2018.

[15] M. Giordani *et al.*, "A tutorial on beam management for 3gpp nr at mmwave frequencies," *IEEE Communications Surveys & Tutorials*, vol. 21, no. 1, pp. 173–196, 2018.

[16] C. K. Anjinappa and I. Guvenc, "Millimeter-wave v2x channels: Propagation statistics, beamforming, and blockage," *IEEE 88th Vehicular Technology Conference (VTC-Fall)*, 2018.

[17] W. Xia *et al.*, "Millimeter wave remote uav control and communications for public safety scenarios," in *2019 16th Annual IEEE International Conference on Sensing, Communication, and Networking (SECON)*, June 2019, pp. 1–7.

[18] K. Antevski *et al.*, "Enhancing edge robotics through the use of context information," in *Proc. Wkshp. Experimentation and Measurements in 5G*, ser. EM-5G'18, 2018, pp. 7–12.

[19] 3GPP, "Radio resource control (RRC); protocol specification," *Technical Specification TS38.300 Project (3GPP)*, 2018.

[20] ——, "TS 38.331 project (3gPP)Radio Resource Control (RRC); protocol specification," 2018.

[21] H. Martikainen *et al.*, "On the basics of conditional handover for 5g mobility," *IEEE 29th Annual International Symposium on Personal, Indoor, and Mobile Radio Communications (PIMRC)*, 2018.

[22] Z. C. Lipton, "A critical review of recurrent neural networks for sequence learning," *ArXiv*, vol. abs/1506.00019, 2015.

[23] F. A. Gers and J. Schmidhuber, "Recurrent nets that time and count," *Proceedings of the IEEE-INNS-ENNS International Joint Conference on Neural Networks. IJCNN 2000. Neural Computing: New Challenges and Perspectives for the New Millennium*, vol. 3, pp. 189–194 vol.3, 2000.

[24] 3GPP, "TR 38.901, study on channel model for frequencies from 0.5 to 100 GHz (release 15) document," Jun. 2018.

[25] ——, "TS 38.213, NR - physical layer procedures for control - (release 15) document," Jun. 2018.

[26] S. H. Ali Shah *et al.*, "Power efficient discontinuous reception in thz and mmwave wireless systems," in *2019 IEEE 20th International Workshop on Signal Processing Advances in Wireless Communications (SPAWC)*, July 2019, pp. 1–5.

[27] I. K. Jain, R. Kumar, and S. Panwar, "Limited by capacity or blockage? a millimeter wave blockage analysis," *Proc. Intl. Teletraffic Congress*, pp. 153–159, 2018.

[28] 3GPP, "TR 38.214,, NR - Physical layer procedures for data - (release 15) document," Jun. 2018.

[29] ——, "TR 38.900, study on channel model for frequency spectrum above 6 GHz release," Jun. 2018.

[30] C. Slezak, A. Dhananjay, and S. Rangan, "60 ghz blockage study using phased arrays," in *2017 51st Asilomar Conference on Signals, Systems, and Computers*, Oct 2017, pp. 1655–1659.

[31] S. H. A. Shah *et al.*, "Beamformed mmwave system propagation at 60 GHz in an office environment," in *2020 IEEE International Conference on Communications (ICC)*, June 2020, pp. 1–7.